

The contribution of cosmic rays to global warming.

T. Sloan¹ and A. W. Wolfendale²

(1) Department of Physics, Lancaster University, UK

(2) Department of Physics, Durham University,
Durham, UK

July 2, 2018

Abstract

A search has been made for a contribution of the changing cosmic ray intensity to the global warming observed in the last century. The cosmic ray intensity shows a strong 11 year cycle due to solar modulation and the overall rate has decreased since 1900. These changes in cosmic ray intensity are compared to those of the mean global surface temperature to attempt to quantify any link between the two. It is shown that, if such a link exists, the changing cosmic ray intensity contributes less than 8% to the increase in the mean global surface temperature observed since 1900.

1 Introduction

There are many claims that cosmic rays (CR) influence the climate significantly, so that some of the Global Warming (GW) seen since industrialisation could be due to the effects of them (e.g.see Dorman 2009, Rao 2011, Veizer 2005, Lee 2003, Weber 2010). The essence of these works is that because the CR intensity has been falling over the last century and that CR could influence cloud formation (Svensmark and Friis-Christensen 1997, Marsh and Svensmark 2000, Svensmark 2007, Svensmark and Calder 2007), a significant contribution to GW could result.

The formation of condensation nuclei of nanometer sizes, on which clouds seed, is not well understood. The standard picture is that such nuclei form on atmospheric impurities such as sulphates, microscopic dust or salt particles (Taylor 2005). A further contribution is possible, namely, through atmospheric ionization as has been shown theoretically by Yu and Yu and Turco (Yu 2002) and experimentally by Enghoff et al (Enghoff et al. 2011). The crucial question is the extent to which ionization from cosmic rays affects the rate of formation of condensation nuclei compared to that provided by the standard known processes. If the effect of CR is significant it will influence GW.

In order to give a quantitative answer to the question of the contribution of the changing CR rate to GW we compare the variation of the galactic CR intensity over the last century to

the observed mean global surface temperature. Previous studies have been made of correlations between various climatological processes and the mean global surface temperature (e.g. Lean and Rind 2008). However, CR have not been explicitly considered and this question is addressed here. Firstly, the long term trend of the CR rate and the global temperature are compared. Secondly, a search is made for an 11 year cycle in the temperature data of a comparable shape to that caused by the solar modulation of the CR intensity.

2 The long term trends of the cosmic ray intensity and temperature

Figure 1 (upper plot) shows the variation of the galactic CR rate in terms of the equivalent Climax neutron monitor rate. The Climax neutron monitor rate is here used as a proxy for the rate of production of atmospheric ionization by galactic CR. The neutron monitor rates have been derived from 1428 to 2005 (McCracken and Beer 2007) directly from the Climax neutron monitor record (1953-2006), from ion chamber data (1933-65) and from the observations of ^{10}Be in ice cores. The lower plot in figure 1 shows the mean global surface temperature anomaly as a function of time (NASA 2011). The CR rate has fallen with time since 1880 as the global temperature has risen. This has been used to postulate that cosmic rays play a significant role in global warming (Rao 2011, Svensmark 2007). A clear 11 year modulation due to solar activity can also be seen in the variation of the CR rate in the upper plot of figure 1.

Figure 2 shows the data from figure 1 with 11 year smoothing applied to illustrate the long term trends (removing the effects of the solar cycle). It can be seen that the CR rate decreased rapidly from 1880 to 1950 when the temperature rise was relatively small. On the other hand the CR rate changed little from 1950-2000 when the temperature rise was bigger (Lockwood and Fröhlich 2007). Hence the variation of the temperature with time matches poorly the variation of the CR rate with time. Such a match would be expected if CR played a significant role in global warming. It can be seen that the CR rate decreased in intensity by $\sim 16\%$ from 1880 to 1952 during which time the mean global temperature rose by $\sim 0.3^\circ$ while from 1952 to 2000 the CR rate decreased by $\sim 3\%$ and the temperature rose by $\sim 0.6^\circ$.

Figure 3 shows the values of the temperature anomalies ΔT , plotted as a function of CR rate, each taken from figure 2. It can be seen that in the early part of the 20th century there was a roughly linear relationship between the two. Linear fits were made to the data in various time ranges starting from 1886. The slopes, $d\Delta T/d\text{CR}$, varied in values from -0.008 to -0.022 $^\circ\text{C}$ per % change in the Climax NM rate as the end year of the fit varies from the year 1930 to 2000. Cycling through each end year in this time range, the mean value of $d\Delta T/d\text{CR}$ was -0.016°C per % change in the Climax NM rate with root mean square deviation of the readings of 0.003. If there is a causal link between CR and the global temperature, this value of $d\Delta T/d\text{CR}$ implies that the 3% change in CR rate observed since 1952 would give a temperature change of $\sim 0.05^\circ\text{C}$. The observed change in temperature since 1952 is $\sim 0.6^\circ\text{C}$. Hence less than $\sim 8\%$ of the observed rise in temperature since 1952 can be ascribed to CR. We take this as an upper limit on the contribution of CR to GW.

3 The 11 year cycle

The CR rates in figure 1 show a clear 11 year cyclic wave due to solar activity whilst such a wave is difficult to discern in the temperature variation. A Fourier analysis was made of each of the variations in figure 1 in order to measure wave amplitudes. The Fourier amplitudes, a , at angular frequency ω were derived from the integral

$$a = \frac{2}{NT} \int_0^{NT} \exp(i\omega t) f(t) dt = \frac{2}{NT} \sum_{bins} \exp(i\omega t) f(t) \delta t \quad (1)$$

where $T = 2\pi/\omega$ is the period at this frequency, N is the number of periods of data analysed, $f(t)$ is the time distribution in bins of width $\delta t=1$ year. Note that the values of a in equation 1 are absolute amplitudes in the same units as the data. These amplitudes will be used throughout this work rather than the more conventional power spectra. There were no missing years in any of the time series. To avoid generating spurious peaks only whole numbers of periods were analysed. This was done in two stages: first from the start of the series and second up to the end of the series, averaging the amplitudes from each stage. In order to reduce noise proportional to the reciprocal of frequency, the data were detrended by fitting simple functions. For the equivalent Climax data a cubic polynomial was fitted and subtracted. For the temperature data an exponential function of time was employed together with a Gaussian shape to account for the anomalous temperature peak at 1942. Optimum fits to the data were obtained using an exponential with time constant 36.5 years and a Gaussian shape centred at 1942 with amplitude 0.21°C and standard deviation 8.67 years. The trend curves are compared with the data in figure 1. Fourier analysis was then carried out on the data with these trend curves subtracted.

Figure 4 shows the results of the Fourier analysis. The solid curve shows the components of the Fourier amplitudes of the temperature data in phase (positive amplitude) or antiphase (negative amplitude) to those measured from an analysis of the equivalent Climax rates (shown in figure 1). To test the sensitivity to the Climax shape the detrended Climax data from figure 1, normalised to temperature waves of different amplitudes, were added to the detrended GISS temperature series (NASA 2011) and the analysis repeated. The dotted and dashed curves in figure 4 show the effects of adding waves normalised to amplitudes of either plus (upper panel) or minus (lower panel) 0.035° and 0.07° , respectively. It can be seen from the solid curves in figure 4 that we do not see a significant shape similar to the equivalent Climax data in the measured amplitudes. This indicates that the amplitude of the 11 year cycle on the global temperatures is small.

To assess the significance of the structures seen in the solid curve in figure 4 randomly generated spectra were passed through the Fourier analysis programs. These were generated with the same root mean square (RMS) noise about the trend curve as measured from the data. The result of analysing 1000 random spectra showed that for periods between 5 and 15 years the RMS deviation of the Fourier amplitudes about zero was $0.0124 \pm 0.0001^\circ\text{C}$. This is to be compared to the value of $0.0115 \pm 0.0023^\circ\text{C}$ observed from the temperature data. These two numbers are equal within the uncertainties showing that the fluctuations in the data are mainly due to noise.

The largest peak observed in the temperature data shown by the solid curves in figure 4 has amplitude -0.04°C and occurs at period 7.5 years. Peaks of the size of this one or greater

occurred in 14% of the random spectra, so this peak is most probably due to noise. Hence no significant structure could be found in the temperature data. In particular, there was no significant structure near to that expected from the CR signal at periods between 10-11 years.

We proceed to assess the minimum detectable Climax-like signal. If a Climax-like signal exists in the temperature data in figure 1, adding in antiphase a normalised measured Climax spectrum will reduce the RMS value of the Fourier amplitudes. The Climax signal necessary to minimise the RMS value of the Fourier amplitudes between periods from 3-12 years in the solid curve of figure 4 was found to be equivalent to a temperature amplitude of -0.023°C . This is taken as the measured temperature wave amplitude although such a small signal cannot be assumed to be real since such values are frequently generated by the random spectra. Climax waves normalised to temperatures of different amplitudes were then added to the random spectra. It was found that, for the addition of a Climax wave normalised to a temperature amplitude of -0.047°C , 10% of the random spectra would have been given a temperature reading closer to zero than the measured value of -0.023°C i.e. a temperature wave of amplitude -0.047°C has a 10% probability to be masked by noise. Hence the minimum detectable temperature amplitude is -0.047°C at 90% confidence level. (or 0.094°C peak to peak). An analysis using the absolute amplitudes without reference to the Climax phase gave a somewhat larger 90% confidence limit on the amplitude of the temperature wave of -0.06°C (or 0.12°C peak to peak). A similar analysis of the positive Climax signals using the phase information shows that waves of amplitude 0.028°C would have been missed in 10% of the cases. Hence the upper limit on the positive temperature amplitude is this value at 90% confidence level.

The average peak to peak amplitude of the 11 year wave on the Climax rate due to solar modulation is 14.7% during 1900-2005. Any link between CR and clouds will cause an antiphase 11 year wave on the temperature. This has been shown above to have amplitude of less than 0.094°C peak to peak. Hence $d\Delta T/d\text{CR}$ is less than 0.0064°C per % change in the Climax rate at 90% confidence level. The observed temperature rise from 1900-2005 is 0.8° and the total change in the Climax NM rate was 11% (figures 1 and 2). Hence the total change in global temperature due to CR must be less than 0.07°C from 1900-2005 which is less than 9% of the observed GW at 90% confidence level. This figure would rise to 11% of the GW if the value of $d\Delta T/d\text{CR}$ without the Climax phase information is used.

4 The effect of time constants or delays

The variation of the CR rate could be made compatible with that of the global temperatures by the introduction of either an integrating time constant or a delay.

The effect of a delay is illustrated in figure 5 which shows the global mean temperature anomaly (Brohan et al., 2006) ¹ as a function of time compared to scaled values of the atmospheric concentration of carbon dioxide (the main green house gas) and those of the Climax rates. It can be seen from the upper plot in figure 5 that if a delay of 35 years is introduced into the CR rates the change beginning in 1940 would resemble the observed temperature rise in the late 20th century. A 35 year timescale could probably be found somewhere in the ocean system

¹The CRU data were used here in order to extend the time series

or even geomagnetically through mantle convection. However, a memory effect of that duration would require the stimulus to be tuned to a very particular regional ocean over-turning. This seems implausible.

The effect of an integrating time constant could also modify the CR rate so that it resembles the temperature variation. This effect is illustrated in the lower plot of figure 5 where the CR rates and the CO₂ concentrations are each passed through an integrating time constant of 50 years. Such a long time constant is necessary to make the change in CR rate resemble the variation of the temperatures. It can be seen from figure 5 that the CO₂ concentration gives a much closer representation of the temperature variation either with or without a time constant than the CR rates.

The effect of a 50 year time constant on the global temperature would be to filter out the influence of the 11 year solar cycle. However, such an effect would also filter out other well known short term variations in the global temperature such as summer to winter changes or day-night variations. Whilst there are effects which introduce delayed warming, such as the thermal inertia of the oceans, the effects of CR on clouds should be on a much shorter time scale than the 50 year time constant necessary to make the CR rates resemble the temperature data. Since this is the main mechanism proposed for CR to affect the climate, the limits for the contribution of CR to GW which we have described in the previous sections seem safe.

5 Discussion of the results

The contribution of cosmic rays to the increase in the mean surface temperature of the Earth during the last century has been assessed by comparing the shapes of the variation in the cosmic ray rate to those of the observed mean global surface temperatures. The long term variation gives an upper limit on the contribution of cosmic rays to GW of less than 8% of the observed increase in temperature. It is difficult to gauge the statistical confidence level of this value since the change in cosmic ray rate is rather uncertain and depends on the precise start date. The result is conservative since if we had chosen the start date to be 1955 rather than 1952 the change in cosmic ray rate would have been zero giving a limit of 0%.

The contribution from the shorter term 11 year variation is shown to be less than 9% of the GW since 1900 at the 90% confidence level. This limit would increase, due to dilution of the 11 year cycle, if the dwell time of condensation nuclei is a few years as required by the analysis of (Weber 2010). Our limit is not inconsistent with the value from (Lean and Rind 2008) who deduced from a linear regression analysis that there was an 11 year wave on the temperature data due to solar insolation with a peak to peak amplitude slightly smaller than our limit.

In conclusion, we deduce that cosmic rays play only a minor part in the global warming observed in the last century (less than 8% of the rise in temperature). Hence standard processes for cloud seeding must be the dominant mechanisms and ionization seeding of clouds can only play a minor part. Finally, using the value of the radiative forcing of 1.6 W/m² derived by the Intergovernmental Panel on Climate Change (IPCC 2007) to produce the observed warming in the last century, the radiative forcing induced by changing cosmic ray rates must be less than 0.14 W/m².

6 Acknowledgement

We thank K. G. McCracken for providing us with the equivalent Climax count rates from the analysis of the direct Climax data, the ion chamber data and the ^{10}Be ice core data. We also thank the Dr. John C. Taylor Charitable Foundation for financial support.

7 References

1. Brohan P., Kennedy J. J., Harris I., Tett S.F.B., and Jones P.D., 2006, Uncertainty estimates in regional and global observed temperature changes: a new dataset from 1850, *J. Geophysical Research* 111, D12106, doi:10.1029/2005JD006548. (available at <http://www.cru.uea.ac.uk/cru/data/temperature/>).
2. Dorman, L., 2009, *The Role of Space Weather and Cosmic Ray Effects in Climate Change*, *Climate Change: Observed Impacts on Planet Earth*, Elsevier.
3. Enghoff M.B., Pedersen J.O.P., Uggerhøj U.I., Paling S.M. and Svensmark H., 2011, Aerosol nucleation induced by a high energy particle beam, *Geophysical Research Letters* 38, LO9805, doi:10.1029/2011GL047036.
4. Hansen, J., Mki. Sato, R. Ruedy, K. Lo, D.W. Lea, and M. Medina-Elizade, 2006: Global temperature change, *Proc. Natl. Acad. Sci.*, 103, 14288-14293, doi:10.1073/pnas.0606291103. (available at <http://data.giss.nasa.gov/gistemp/graphs/>)
5. IPCC 2007, 4th Assessment Report of the IPCC (WG1 Figure SPM2).
6. Lean J.L. and Rind D.H., 2008, How natural and anthropogenic influences alter global and regional surface temperatures: 1889 to 2006. *Geophysical Research Letters* **35** L18701, DOI:10.1029/2008GL034864.
7. Lee S.H. et al., 2003, Particle formation by ion nucleation in the upper troposphere and lower stratosphere, *Science* **298**, 172.
8. Lockwood M. and Frölich C., 2007 Recent oppositely directed trends in solar climate forcings and the global mean surface air temperature, *Proc. Roy. Soc.* **A463** no. 2086, 2447-2460 doi: 10.1098/rspa.2007.1880.
9. Marsh N. and Svensmark H., 2000, Low cloud properties influenced by cosmic rays, *Phys. Rev. Letts.* **85**, 5004.
10. McCracken, K.G. and Beer, J., 2007, Long-term changes in the cosmic ray intensity at Earth, 1428 - 2005, *Journ. Geophys. Res.* 112, A 10101.
11. NASA 2011, available at <http://data.giss.nasa.gov/gistemp/>
12. NOAA 2011, Tans P. and Keeling R. (Scripps Institution of Oceanography). The CO₂ data are available at www.esrl.noaa.gov/gmd/ccgg/trends/

13. Rao, U.R., 2011, Contributions of changing galactic cosmic ray flux to global warming, *Current Science*, 100, 2, 223.
14. Svensmark H. and Friis-Christensen E., 1997, Variation of cosmic ray flux and global cloud coverage: a missing link in sun-climate relationships. *J. Atmospheric and Solar Terrestrial Physics* **59** 1225.
15. Svensmark H., 2007, Cosmoclimatology: a new theory emerges, *New Reviews in Astronomy and Geophysics* **48** 18.
16. Svensmark H. and Calder N., 2007, *The Chilling Stars: A New Theory of Climate Change*, (published by Icon Books).
17. Taylor F.W., 2005, *Elementary Climate Physics*, ISBN 978 0 19 856733 2. Oxford University Press.
18. Veizer J., 2005, Celestial Climate Driver: a perspective from four billion years of the carbon cycle, *GeoScience Canada*, **32** Number 1, 13.
19. Weber W., 2010 Strong signature of the active Sun in 100 years of terrestrial insolation data, *Ann. Phys.(Berlin)* No. 6 **522** 372-381 /DOI 10.1002/andp.201000019.
20. Yu F., 2002, Altitude Variation of cosmic ray production of aerosols: Implications for global cloudiness and climate, *Journal of Geophysical Research*, **107** number A7, 10.1029/2001JA000248.

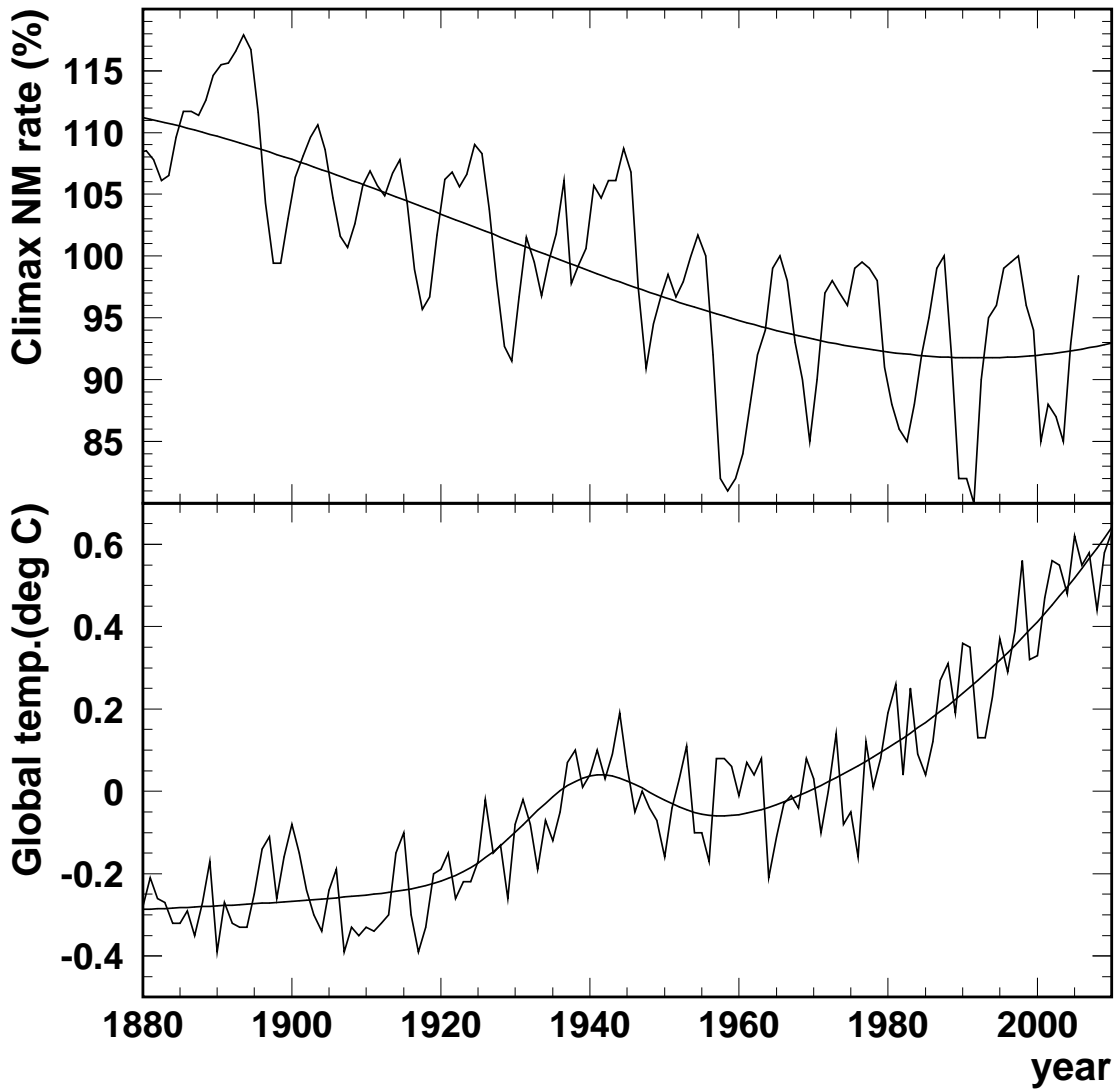


Figure 1: **Upper panel** shows the equivalent Climax neutron monitor rate (McCracken and Beer 2007) against time. **Lower panel** shows the mean global surface temperature from the GISS data against time. Both data sets are yearly averages. The smooth curves show the fitted functions used to detrend the data (see section 3).

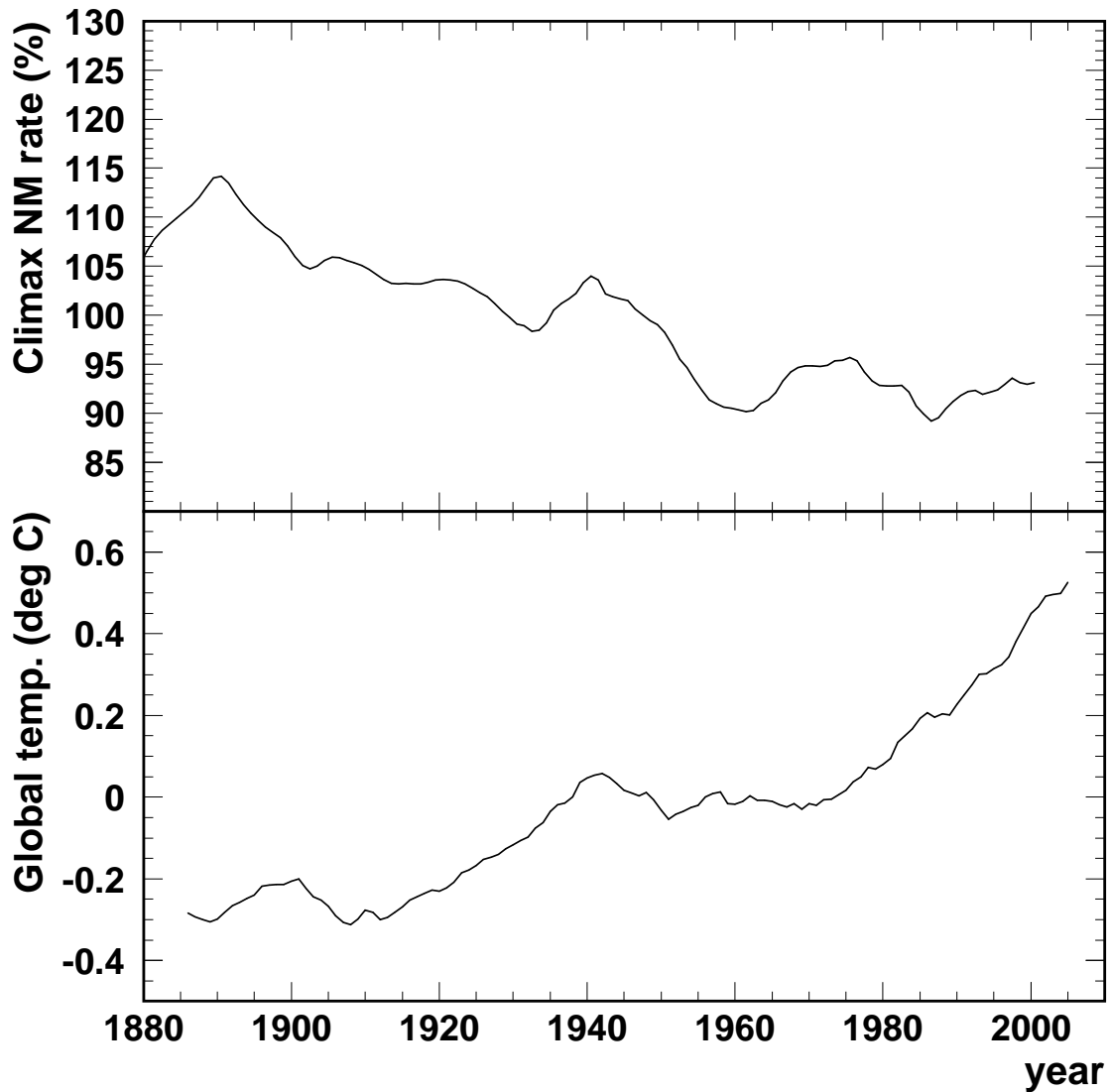


Figure 2: **Upper panel** shows the equivalent Climax neutron monitor rate (McCracken and Beer 2007) against time with 11 year smoothing to illustrate the trend and smooth out the effects of the solar cycle. **Lower panel** shows the mean global surface temperature from the GISS data against time with the same 11 year smoothing applied.

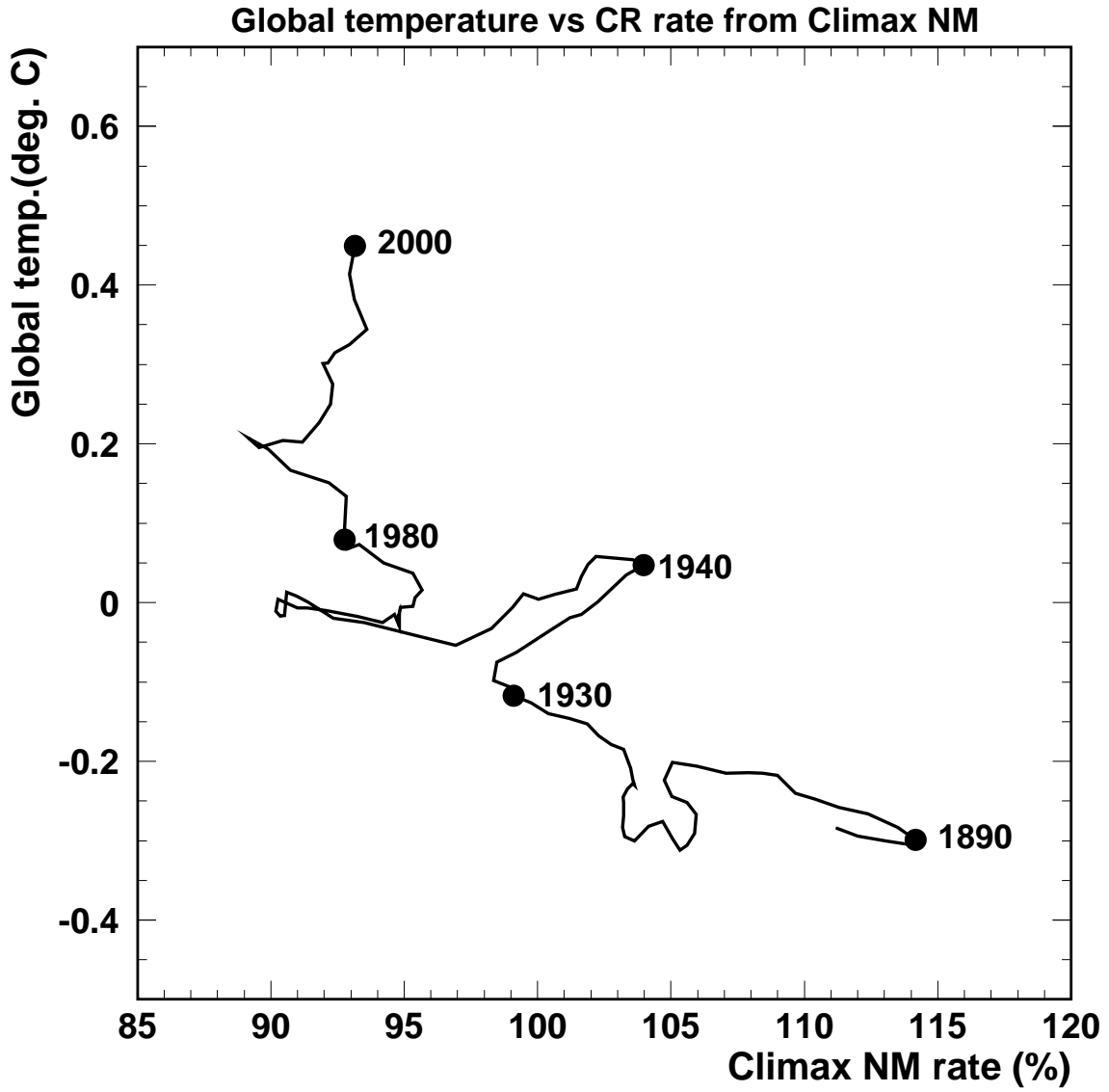


Figure 3: The data from figure 2 plotted as equivalent Climax neutron monitor rate against temperature anomaly. The solid points correspond to the years marked.

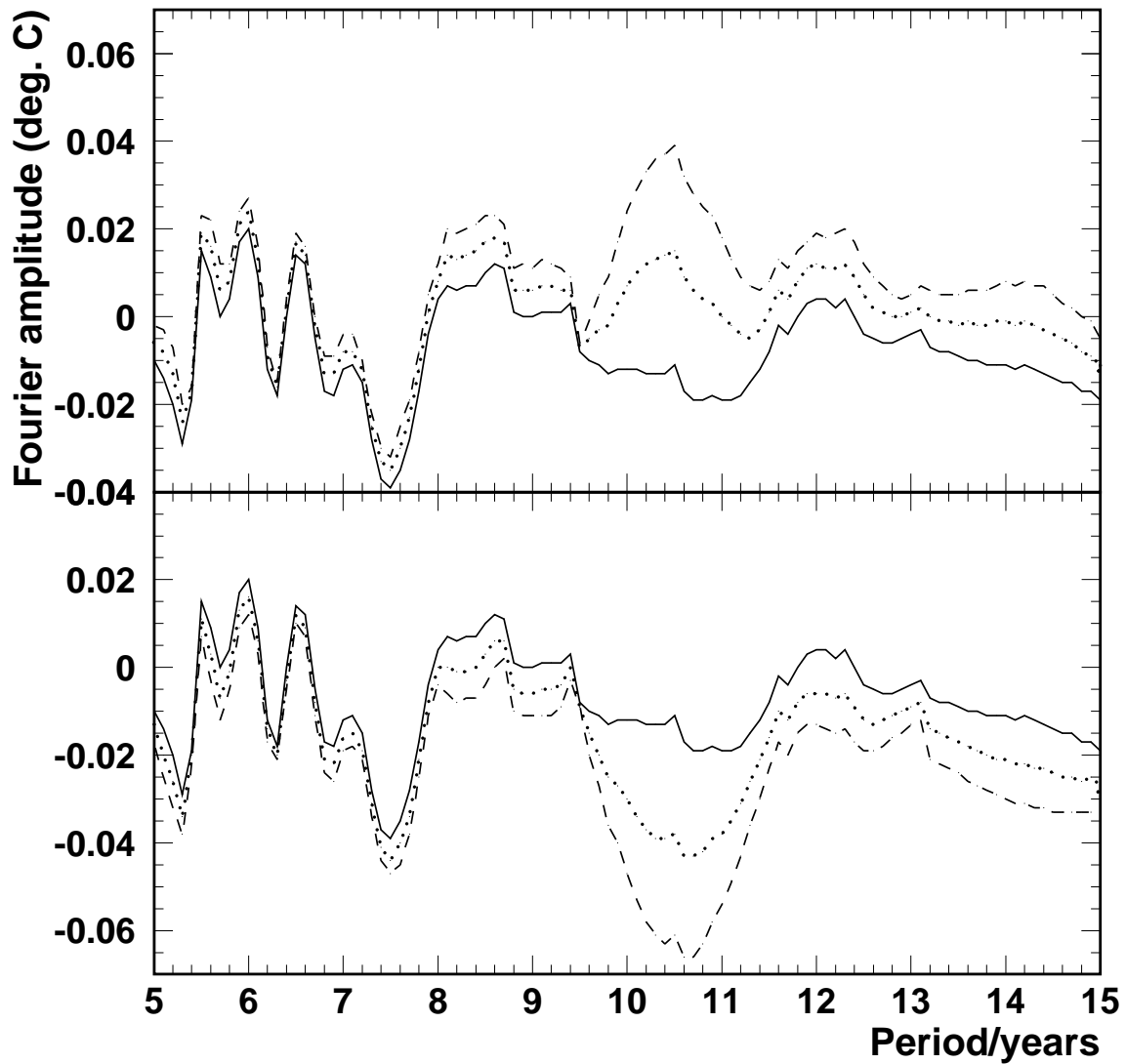


Figure 4: Fourier amplitude components in $^{\circ}\text{C}$ in phase with the equivalent Climax neutron monitor wave as a function of wave period. The solid curves show the Fourier components of the the GISS temperature measurements shown in figure 1. The dotted and dashed curves show the results of the analysis applied to these temperatures with equivalent Climax data normalised to temperature waves of amplitude 0.035 and 0.07°C , respectively, added directly to the temperature data (plus in the upper panel, minus in the lower panel).

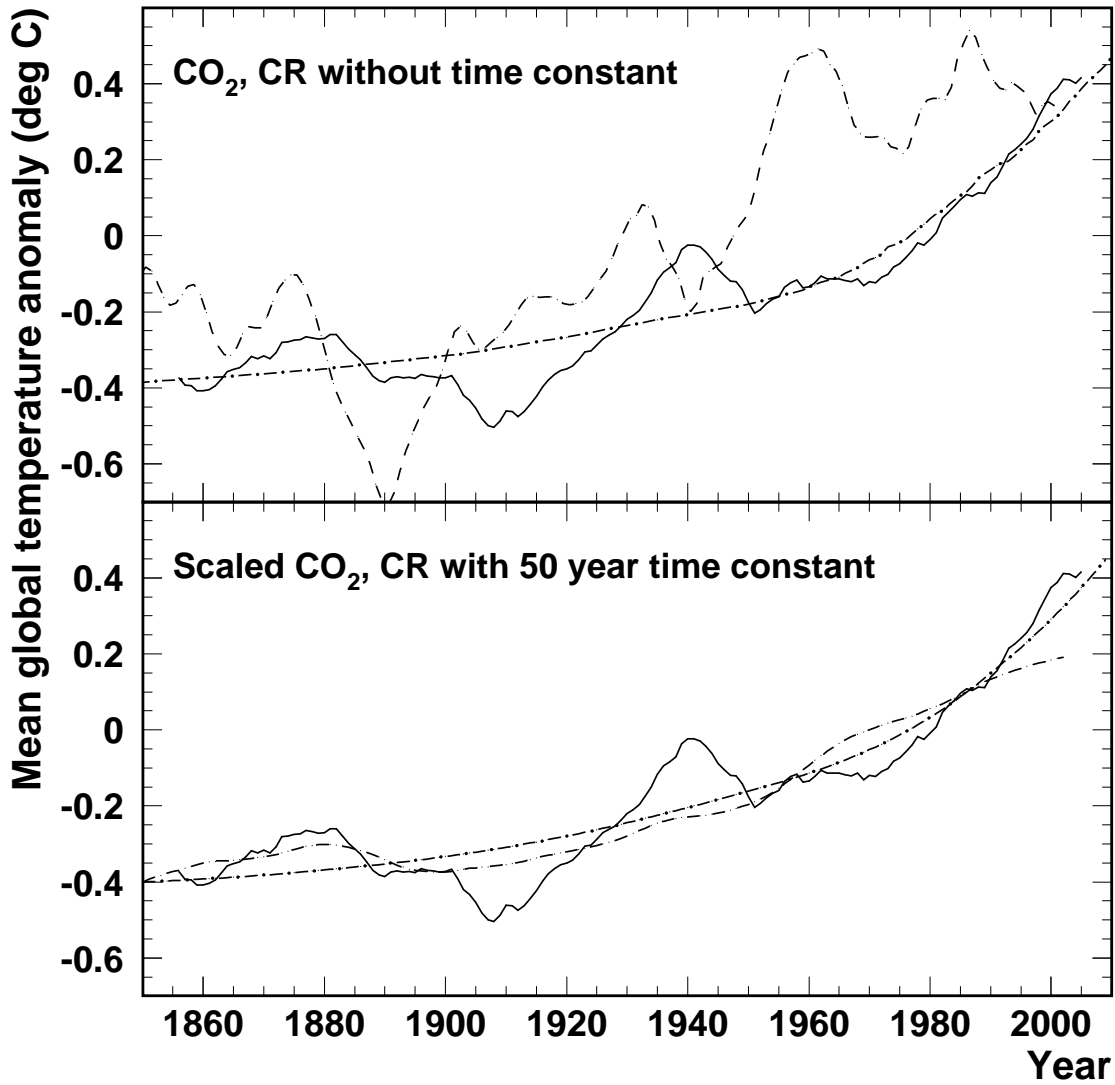


Figure 5: Comparison of the mean global surface temperature anomalies (solid curves) with the scaled measured CR rates (dashed curves) and CO_2 concentrations (dash-dotted curves). The CO_2 measurements are scaled so that $T_{CO_2} = k_{CO_2}(CO_2 - 285) - 0.4$ and the CR measurements so that $T_{CR} = k_{CR}(100 - CL)$ where k_{CO_2} and k_{CR} are normalising constants, CO_2 is the concentration of carbon dioxide in the atmosphere in ppmv (NOAA 2011) and CL are the Climax rates (McCracken and Beer 2007). In the upper plot the scaled CO_2 and CR measurements were plotted directly with $k_{CO_2}=0.0083$ and $k_{CR}=0.05$. In the lower plots the CO_2 and Climax rates were passed through an integrating time constant of 50 years. The values of the constants to achieve a reasonable representation of the data in this case are $k_{CO_2}=0.0175$ and $k_{CR}=0.52$.